3. LINEAR, COUPLED LUMPED ELEMENTS

Coupled lumped elements appear primarily in the M-phase π-circuit representation of transmission lines, in the representation of transformers as coupled impedances, and as source impedances in cases where positive and zero sequence parameters are not equal.

3.1 Coupled Resistances [R]

Coupled resistances, in the form of branch resistance matrices [R], appear primarily

(a) as part of the series impedance matrix in M-phase nominal π-circuits,

(b) as long line representations in lightning surge studies if no reflections come back from the remote end during the duration t_{max} of the study.

The diagonal elements of [R] are the self resistances, and the off-diagonal elements are the mutual resistances. The off-diagonal terms in the series resistance matrix of an M-phase line are caused by the presence of the earth as a potential current return path. The earth is not modelled as a conductor as such; instead, it is used as a reference point for measuring voltages. If it were explicitly modelled as a conductor, its equation for a three-phase line could have the form

$$-\frac{dV_E}{dx} = Z'_{EA}I_A + Z'_{EB}I_B + Z'_{EC}I_C + Z'_{EE}I_E$$

Since the voltages are measured with respect to earth, $V_E = 0$, and therefore,

$$I_E = -\frac{Z'_{EA}}{Z'_{EE}}I_A - \frac{Z'_{EB}}{Z'_{EE}}I_B - \frac{Z'_{EC}}{Z'_{EE}}I_C$$

which, when inserted into the voltage drop equations for the phases A, B, C, produces

$$-\frac{dV_A}{dx} = \left(Z'_{AA} - \frac{Z'_{AE}Z'_{EA}}{Z'_{EE}}\right)I_A + \left(Z'_{AB} - \frac{Z'_{AE}Z'_{EB}}{Z'_{EE}}\right)I_B + \left(Z'_{AC} - \frac{Z'_{AE}Z'_{EC}}{Z'_{EE}}\right)I_C$$

and similar for B, C. This is the form used in M-phase π-circuits, with earth being an implicit, rather than explicit, current conductor. Assuming purely inductive coupling $Z'_{ik} = jX'_{ik}$, the terms $Z'_{AE}Z'_{EB}/Z'_{EE}$ etc. will obviously contain real parts since the self impedance of the earth Z'_{EE} contains a real part. Whether the real part thus produced can strictly be treated as a resistance for all frequencies is open to debate, as explained in Section 4.1.2.4.

The EMTP automatically converts a long line with distributed parameters into a shunt resistance matrix [R] if

(1) $\tau > t_{max}$ for all M modes[1] of the M-phase line,

[1]Modes are explained in Section 4.1.5.

(2) zero initial conditions.

This representation is simply an M-phase generalization of the single-phase case discussed in Section 2.1. For the high-frequency lossless line model, which is often used in lightning surge studies and described in more detail in Section 4.1.5.2, this shunt resistance matrix has the elements

$$R_{ii} = 60 \ln \frac{2h_i}{r_i}, \quad R_{ik} = 60 \ln \frac{D_{ik}}{d_{ik}} \tag{3.1}$$

with h_i = average height above ground, r_i = conductor radius, D_{ik} = distance from conductor i to image of conductor k, d_{ik} = direct distance between conductors i and k. These are the well-known self and mutual surge impedances of an M-phase line [8].

The equations for coupled resistances

$$[i_{km}(t)] = [R]^{-1}\{[v_k(t)] - [v_m(t)]\} \tag{3.2}$$

are solved accurately by the EMTP, as long as [R] is non-singular and not extremely ill-conditioned. In all cases known so far, [R] is symmetric, and the EMTP has therefore been written in such a way that it only accepts symmetric matrices [R].

The EMTP does not have an input option for coupled resistances by themselves; instead, they must be specified as part of the M-phase nominal π-circuit of Section 3.4, with L and C left zero. For long lines with $\tau > t_{max}$ and zero initial conditions, the EMTP converts the distributed-parameter model internally to the form of Eq. (3.2). Since [R] is symmetric, the EMTP stores and processes the elements of these and all other coupled-branch matrices as one-dimensional arrays in and above the diagonal (e.g. R_{11} stored in X(1), R_{12} in X(2), R_{22} in X(3), R_{13} in X(4), etc.).

3.1.1 Error Analysis

As already mentioned, [R] must be non-singular if a resistance matrix is read in. If its inverse $[R]^{-1}$ is read in, then this requirement can be dropped, since $[R]^{-1}$ is allowed to be singular without causing any problems. Also, the resistances shouldn't be so small that $[R]^{-1}$ becomes so large that it "swamps out" the effect of other connected elements, as mentioned in Section 2.1.1. On the other hand, very small values of $[R]^{-1}$ are acceptable (see "very large resistances" in Section 2.1.1).

3.1.2 Insertion of Coupled Branches into Nodal Equations

Since coupled branches have not been discussed in the introduction to the solution methods, their inclusion into the system of nodal equations shall briefly be explained. Assume that three branches ka-ma, kb-mb, kc-mc are coupled (Fig. 3.1). In forming the nodal equation for node ka, the current $i_{ka,ma}$ is needed,

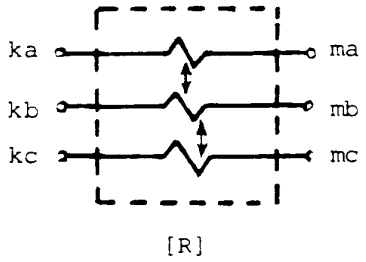

Fig. 3.1 - Three coupled resistances

$$i_{ka,ma} = G_{aa}^{branch}\left(v_{ka} - v_{ma}\right) + G_{ab}^{branch}\left(v_{kb} - v_{mb}\right) + G_{ac}^{branch}\left(v_{kc} - v_{mc}\right)$$

with G^{branch}_{ik} being elements of the branch conductance matrix $[R]^{-1}$. This means that in the formation of the nodal equation for node ka, G^{branch}_{aa} enters into element $G_{ka,ka}$ of the nodal conductance matrix in Eq. (1.8a), $-G^{branch}_{aa}$ into $G_{ka,ma}$, G^{branch}_{ab} into $G_{ka,kb}$, $-G^{branch}_{ab}$ into $G_{ka,mb}$, etc. If this is done systematically, the matrix $[R]^{-1}$ will be added to two diagonal blocks, and subtracted from two off-diagonal blocks of the nodal conductance matrix [G], as indicated in Fig. 3.2. Unfortunately, rows and columns ka, kb, kc and ma, mb, mc do not follow each other that neatly, and the entries in [G] will therefore be all over the place, but this is simply a programming task. It is worth pointing out that the entry of coupled branches into the nodal conductance matrix can always be explained with an equivalent network of uncoupled elements. For three coupled resistances, the equivalent network with uncoupled elements would contain 15 uncoupled resistances (see Fig. 7 in Chapter II of [26]). Such equivalent networks with

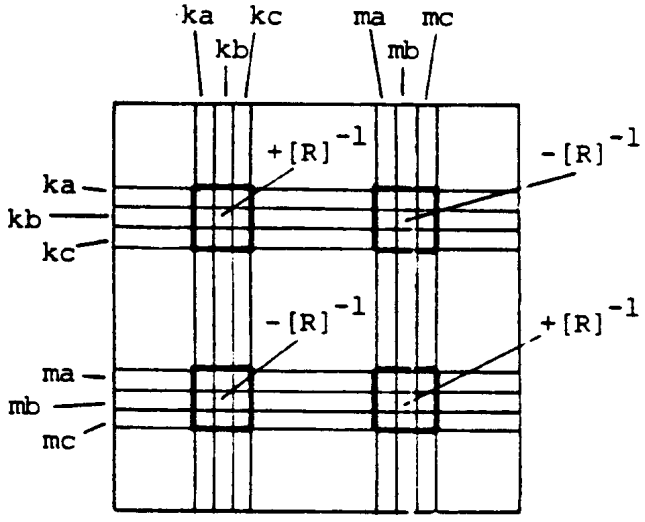

Fig. 3.2 - Contributions of three coupled branches to the nodal conductance matrix

uncoupled elements are useful for assessing the sparsity of a matrix, but they can be misleading by seemingly indicating galvanic connections where none exist. For example, the steady-state branch equations for two-winding transformers, which are well known from power flow and short-circuit analysis,

$$\begin{bmatrix} I_{ka,ma} \\ I_{kb,mb} \end{bmatrix} = \begin{bmatrix} Y & -tY \\ -tY & t^2Y \end{bmatrix} \begin{bmatrix} V_{ka} & -V_{ma} \\ V_{kb} & -V_{mb} \end{bmatrix} \tag{3.3}$$

simply imply the connection of Fig. 3.3(a), and nothing more. The equivalent network with uncoupled elements is shown in Fig. 3.3(b), which produces the well-known transformer model of Fig. 3.3(c) if nodes ma and mb are grounded.

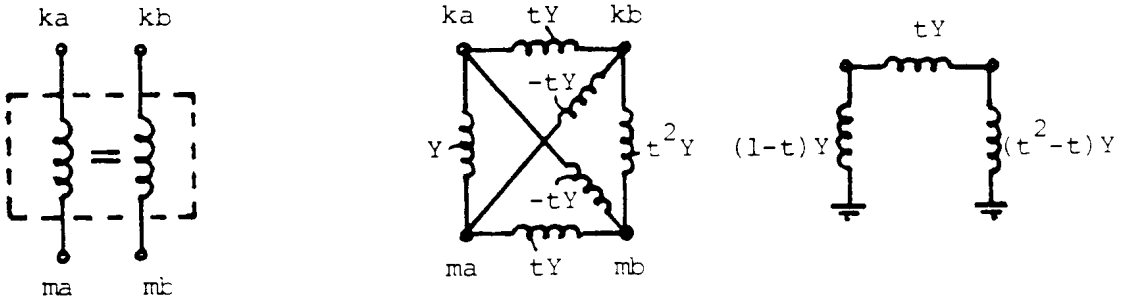

(a) Coupled elements (b) Uncoupled elements (c) Uncoupled elements with nodes ma and mb grounded

Fig. 3.3 - Two-winding transformer as two coupled branches

3.1.3 Example for Coupled Resistance

Assume that a lightning stroke, represented by a current source i(t), hits phase A of a three-phase line (Fig. 3.4). Let us then find the voltage build-up in all 3 phases over a time span

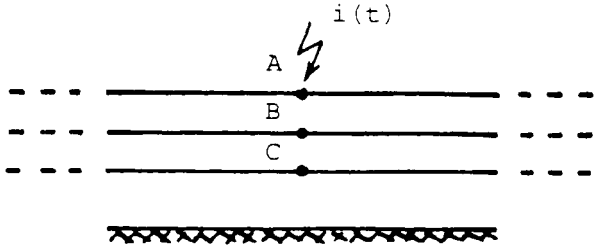

Fig. 3.4 - Lightning stroke to phase A of a three-phase line

during which reflections have not yet come back from the remote ends of the line, using the high-frequency lossless line model of Eq. (3.1). Assume a flat tower configuration typical of 220 kV lines, with an average height above ground = 12.5 m, spacing between conductors = 7.58 m, and conductor radius 14.29 mm. Then from Eq. (3.1),

$$[R] = \begin{bmatrix} 448.02 & 74.24 & 39.41 \\ 74.24 & 448.02 & 74.24 \\ 39.41 & 74.24 & 448.02 \end{bmatrix} \Omega$$

The left as well as the right part of the line is then represented by [R] connected from A, B, C to ground, and the

voltages become

$$v_A(t) = 224.01\ i(t)$$
$$v_B(t) = 37.12\ i(t)$$
$$v_C(t) = 19.71\ i(t)$$

or 16.6% of v_A appears in phase B, and 8.8% in phase C. An interesting variation of this case is the calculation of the effect which this lightning stroke has on the equipment in a substation. Assume that the travel time τ between the stroke location and the substation is such that no reflection comes back from the stroke location during the time t_{max} of the study, with the time count starting when the waves hit the substation (Fig. 3.5). In such cases, the waves coming into the substation can be represented as a three-phase voltage source with amplitudes equal to twice the value of the voltages at the stroke location, behind the resistance matrix [R]. This, in turn, can be converted to a current source in parallel with a shunt resistance matrix [R]. Since

$$[v_{source}] = 2 \cdot \frac{1}{2}[R]\begin{bmatrix} i(t) \\ 0 \\ 0 \end{bmatrix}$$

it follows that the equivalent current source injected into the substation simply becomes equal to the lightning current at the stroke location [i(t), 0, 0] which together with the shunt resistance matrix [R], represents the waves coming into the substation as long as no reflections have come back yet from the stroke location.

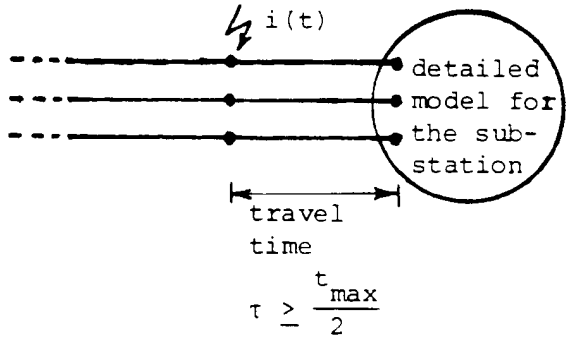

(a) Network configuration

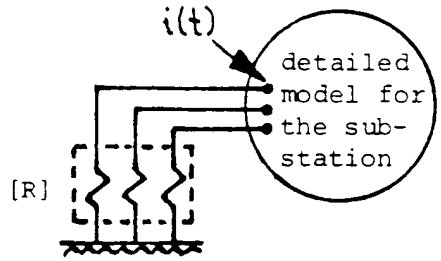

(b) Equivalent network for line and lightning stroke

Fig. 3.5 - Waves coming into substation

3.2 Coupled Inductances [L]

Coupled inductances, in the form of branch inductance matrices, are used to represent magnetically coupled circuits, such as

(a) inductive part of transformers,

(b) inductive part of source impedances in three-phase Thevenin equivalent circuits for the "rest of the system" when positive and zero sequence parameters differ,

(c) inductive part of M-phase nominal π-circuits.

The diagonal elements of [L] are the self inductances, and the off-diagonal elements are the mutual inductances. In all cases known so far, [L] is symmetric, and the EMTP only accepts symmetric matrices, with the storage scheme described in the last paragraph before Section 3.1.1.

The source impedances mentioned earlier under (b) above are often specified as positive and zero sequence parameters Z_{pos}, Z_{zero} which can be converted to self and mutual impedances

$$Z_s = \frac{1}{3}\left(2Z_{pos} + Z_{zero}\right), \qquad Z_m = \frac{1}{3}\left(Z_{zero} - Z_{pos}\right) \tag{3.4}$$

of the coupled impedance matrix

$$[Z] = \begin{bmatrix} Z_s & Z_m & Z_m \\ Z_m & Z_s & Z_m \\ Z_m & Z_m & Z_s \end{bmatrix} \tag{3.5}$$

Of course, these self and mutual impedances can in turn be converted back to sequence parameters,

$$Z_{pos} = Z_s - Z_m , \qquad Z_{zero} = Z_s + 2Z_m \tag{3.6}$$

For a generalization of this data conversion to any number of phases M, see Eq. (4.60) in Section 4.1.3.2.

The equations for coupled inductances between a set of nodes ka, kb,… and a set of nodes ma, mb,… (Fig. 3.6) are solved accurately in the ac steady-state solution with

$$[I_{km}] = \frac{1}{j\omega}[L]^{-1}\{[V_k] - [V_m]\} \tag{3.7}$$

The only precaution to observe is that $[L]^{-1}$ should not be extremely large, for reasons explained in Section 2.1.1.

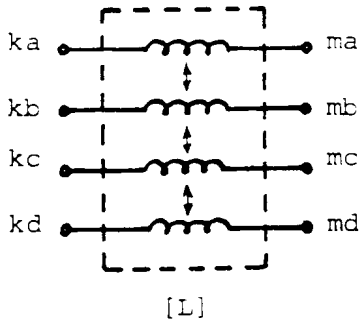

Fig. 3.6 - Four coupled inductances

For the transient simulation, Eq. (2.6) and (2.7) for the scalar case are simply generalized for the matrix case, which produces the desired branch equations

$$[i_{km}(t)] = \frac{\Delta t}{2}[L]^{-1}\{[v_k(t)] - [v_m(t)]\} + [hist_{km}(t-\Delta t)] \tag{3.8}$$

with the history term $[hist_{km}(t - \Delta t)]$ known from the solution at the preceding time step,

$$[hist_{km}(t-\Delta t)] = [i_{km}(t-\Delta t)] + \frac{\Delta t}{2}[L]^{-1}\{[v_k(t-\Delta t)] - [v_m(t-\Delta t)]\} \tag{3.9}$$

Just as in the uncoupled case, Eq. (3.8) can be represented as an equivalent resistance matrix $[R_{equiv}] = (2/\Delta t)[L]$, in parallel with a vector $[hist_{km}(t - \Delta t)]$ of known current sources. The matrix $[R_{equiv}]^{-1}$ enters into the nodal

conductance matrix of the transient solution in the same way as described in Section 3.1.2 (for the steady-state solution, simply replace $[R_{equiv}]^{-1}$ by $(1/j\omega)[L]^{-1}$). While the current source $hist_{km}$ of an uncoupled inductance enters only into two components k and m of the right-hand side in Eq. (1.8b), the vector $[hist_{km}]$ must now be subtracted from components ka, kb, kc,…, and added to components ma, mb, mc,….

Once all the node voltages have been found at a particular time step at instant t, the history term of Eq. (3.9) must be updated for each group of coupled inductances. This could be done recursively with the matrix equivalent of the scalar equation (2.8). The EMTP does not have an input option for coupled inductances alone; instead, they must be specified as part of the M-phase nominal π-circuit of Section 3.4, where the updating formulas used by the EMTP are discussed in more detail.

There are situations where [L] may not exist, but where $[L]^{-1}$ can be specified as a singular matrix. Such an example is the transformer model of Eq. (3.3). If resistances are ignored, Eq. (3.3) can be used for transient studies with

$$[L]^{-1} = j\omega \begin{bmatrix} Y & -tY \\ -tY & t^2Y \end{bmatrix} \tag{3.10}$$

where Y = 1/(jX), with X being the short-circuit input reactance of the transformer measured from winding ka-ma. It is therefore advisable to have input options for $[L]^{-1}$ as well as for [L], as further discussed in Section 3.4.2.

3.2.1 Error Analysis

The errors are the same as for the uncoupled inductance, that is, the ratio $\tan(\omega\,\Delta t/2)/(\omega\,\Delta t/2)$ of Eq. (2.17) applies to every element in the matrix [L], or its reciprocal to every element in $[L]^{-1}$. The stub-line representation of Fig. 2.9 becomes an M-phase stub-line, if M is the size of the matrix [L]. There is no need to use modal analysis for this stub-line because all travel times are equal, as mentioned in Section 4.1.5.2. In that case, the single-phase line equations can be generalized to M-phase line equations by simply replacing scalars with matrix quantities. Eq. (2.9), (2.12) and (2.14) therefore become

$$\mathcal{L}[L'] = [L], \qquad [Z] = \frac{2}{\Delta t}[L], \qquad \textit{and} \quad \mathcal{L}[C'] = \left(\frac{\Delta t}{2}\right)^2 [L]^{-1}$$

3.2.2 Damping of "Numerical Oscillations" with Coupled Parallel Resistances

Again, the explanations of Section 2.2.2 for the uncoupled inductance are easily generalized to the matrix case if all elements of [L] are to have the same ratio R_p/L. Since $[L]^{-1}$ is used in Eq. (3.8), it is preferable to express the parallel resistances in the form of a conductance matrix, e.g., with Alvarado's recipe of Eq. (2.23),

$$[G_p] = 0.15\frac{\Delta t}{2}[L]^{-1} \tag{3.11}$$

If $[L]^{-1}$ is singular, $[G_p]$ would be singular as well, but the singularity would not cause any problems. If the coupled

inductances go from nodes ka, kb,…to nodes ma, mb,… (Fig. 3.6), then [G_p] would be connected in the same way from nodes ka, kb,… to nodes ma, mb,…

3.2.3 Physical Reasons for Coupled Parallel Resistances

The reasons are the same as those listed in Section 2.2.3 in those situations in which the single-phase case can be generalized to the M-phase case.

3.2.4 Example for Network with Coupled Inductances

Let us go back to the example of the single-phase-to-ground fault described in Section 2.2.4, but treat it as a three-phase Thevenin equivalent circuit now, with coupled resistances and inductances (Fig. 3.7). Assume that Z_{pos} = 0.02 + j0.404 p.u. and Z_{zero} = 0.5 + j1.329 p.u., or with Eq. (3.4) Z_s = 0.18 + j0.712 p.u., Z_m = 0.16 + j0.308 p.u. There are three voltage sources now,

$$v_{A-SOURCE} = V_{\max}\sin(\omega t)$$

$$v_{B-SOURCE} = V_{\max}\sin(\omega t - 120°)$$

$$v_{C-SOURCE} = V_{\max}\sin(\omega t + 120°)$$

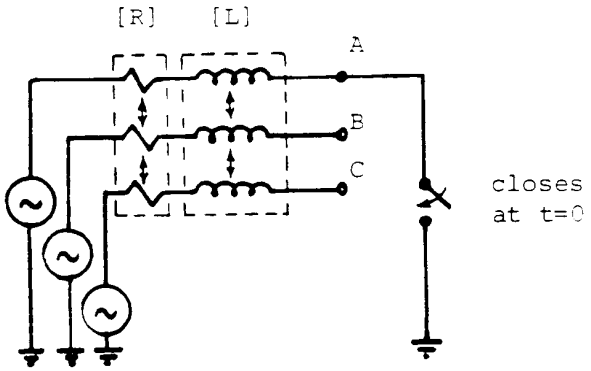

Fig. 3.7 - Single-phase-to-ground fault with three-phase Thevenin equivalent circuit

With the same values of R_s and L_s as in Section 2.2.4, the fault current will be identical with the curves of Fig. 2.21(b) and (c). In addition, we can now obtain the overvoltages in the unfaulted phases B and C, which are shown in Fig. 3.8.

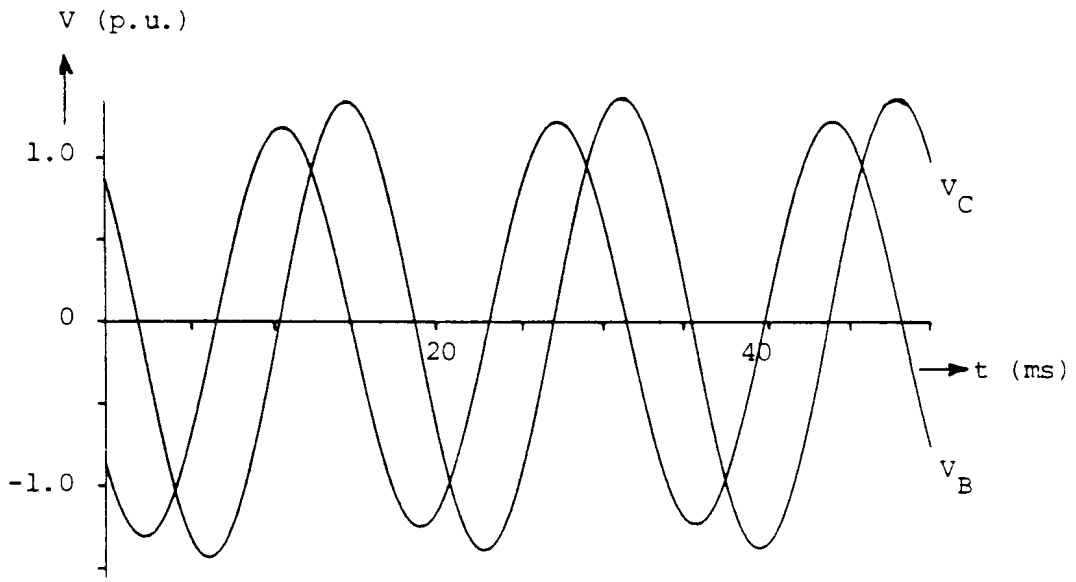

Fig. 3.8 - Overvoltages in unfaulted phases B and C

The steady-state solution can of course be easily obtained from the phasor equations

$$\begin{bmatrix} V_A \\ V_B \\ V_C \end{bmatrix} = \begin{bmatrix} V_{A-SOURCE} \\ V_{B-SOURCE} \\ V_{C-SOURCE} \end{bmatrix} - \begin{bmatrix} Z_s & Z_m & Z_m \\ Z_m & Z_s & Z_m \\ Z_m & Z_m & Z_s \end{bmatrix} \begin{bmatrix} I_A \\ 0 \\ 0 \end{bmatrix} \tag{3.12a}$$

The first row produces, with $V_A = 0$,

$$I_A = \frac{V_{A-SOURCE}}{Z_s} \tag{3.12b}$$

and the second the third rows produce the voltage changes in the unfaulted phases

$$\Delta V_B = \Delta V_C = -\frac{Z_m}{Z_s} V_{A-SOURCE} \tag{3.12c}$$

If these voltage changes are shown in a phasor diagram (Fig. 3.9), then it becomes obvious why the overvoltages in phases B and C are unequal, unless the ratio Z_m/Z_s is a real (rather than complex) number. In the latter case the dotted changes become vertical in B and C in Fig. 3.9, and the overvoltages become equal.

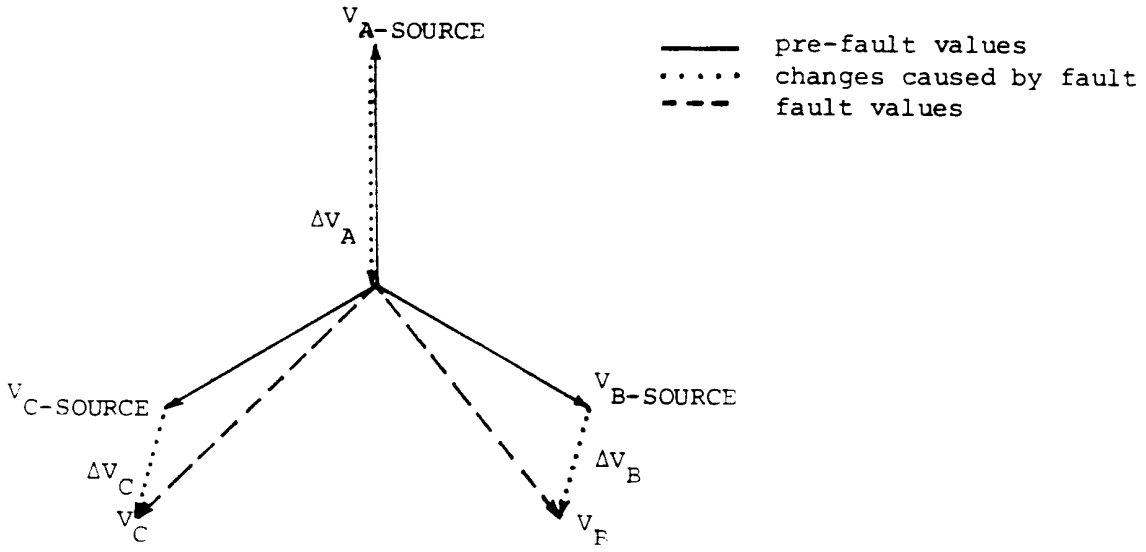

Fig. 3.9 - Phasor diagram of voltage changes caused by single-phase-to-ground fault

3.3 Coupled Capacitances [C]

Coupled capacitances, in the form of branch capacitance matrices, appear as the shunt elements of M-phase nominal π-circuits (Fig. 3.10). One could argue that the capacitances are not really coupled, since they appear as 6 uncoupled capacitances in Fig. 3.10. However, the same argument can be made for coupled resistances and inductances, as explained in Fig. 3.3 of Section 3.1.2, and the fact remains that the shunt capacitances of M-phase lines appear as matrix quantities in the derivation of the equations.

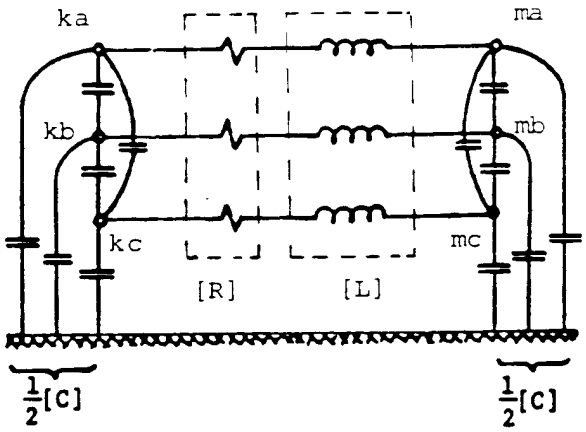

Fig. 3.10 - Three-phase nominal π-circuit

Since the only known application of coupled capacitances is as shunt elements of M-phase nominal π-circuits, the EMTP accepts them only in that form, that is, as equal branch capacitance matrices 1/2 [C] at each end of the π-circuit, from nodes ka, kb,... to ground, and from nodes ma, mb,... to ground. In all cases, [C] is symmetric, and this symmetry is exploited with the storage scheme described in the last paragraph before Section

3.1.1. The diagonal element C_{kaka} of [C] is the sum of all capacitances between phase a and the other phases b, c,… as well as between phase a and ground, whereas the off-diagonal element C_{kakb} is the negative value[2] of the capacitance between phases a and b.

Sometimes, shunt capacitances of three-phase lines are specified as positive and zero sequence parameters C_{pos}, C_{zero}, which can be converted to the diagonal and off-diagonal elements

$$C_s = \frac{1}{3}(2C_{pos} + C_{zero}) \ , \quad C_m = \frac{1}{3}(C_{zero} - C_{pos}) \tag{3.13}$$

of the coupled capacitance matrix

$$[C] = \begin{bmatrix} C_s & C_m & C_m \\ C_m & C_s & C_m \\ C_m & C_m & C_s \end{bmatrix} \tag{3.14}$$

C_m must be negative because the off-diagonal element is the negative value of the coupling capacitance between two phases, therefore, $C_{zero} < C_{pos}$. For a generalization of this data conversion to any number of phases M, see Eq. (4.61) in Section 4.1.3.2.

The steady-state equations for coupled capacitances in the shunt connection of Fig. 3.10, and with the factor 1/2, are

$$[I_{k0}] = \frac{1}{2} j\omega [C][V_k], \qquad [I_{m0}] = \frac{1}{2} j\omega [C][V_m] \tag{3.15}$$

with subscripts "k0" and "m0" indicating that the currents flow from nodes ka, kb,… to ground ("0"), and from nodes ma, mb,… to ground. Eq. (3.15) is solved accurately in the steady-state solution. The only precaution to observe is that ω[C] should not be extremely large, for reasons explained in Section 2.1.1, but this is very unlikely to occur in practice anyhow.

For the transient simulation, Eq. (2.29) and (2.30) are again generalized for the matrix case, which produces the desired branch equations (taking care of the factor 1/2!),

$$[i_{k0}(t)] = \frac{1}{\Delta t}[C][v_k(t)] + [hist_{k0}(t-\Delta t)] \tag{3.16}$$

with the history term $[hist_{k0}(t - \Delta t)]$ known from the solution at the preceding time step,

---

[2]It might be worthwhile to have the EMTP check for the negative sign, and automatically make it negative, with an appropriate warning message, in cases where the negative sign was forgotten. The writer is not aware of any situation in which the off-diagonal element would not be negative.

$$[hist_{k0}(t-\Delta t)] = -\frac{1}{\Delta t}[C][v_k(t-\Delta t)] - [i_{k0}(t-\Delta t)] \tag{3.17}$$

The equations for the shunt capacitance 1/2 [C] at the other end (nodes ma, mb,…) are the same if subscript k is replaced by m. As in the uncoupled case, Eq. (3.16) can be represented as an equivalent resistance matrix $\Delta t[C]^{-1}$, in parallel with a vector $[hist_{km}(t - \Delta t)]$ of known current sources. The matrix $1/\Delta t$ [C] enters into the nodal conductance matrix of the transient solution only in the diagonal block of rows and columns ka, kb,… and in the diagonal block of rows and columns ma, mb,… (Fig. 3.2), because of the shunt connection, while the vector $[hist_{k0}]$ must be subtracted from components ka, kb,… (analogous for $[hist_{m0}]$).

Once all the node voltages have been found at a particular time step at instant t, the history term of Eq. (3.17) is updated recursively,

$$[hist_{k0}(t)] = -\frac{2}{\Delta t}[C][v_k(t)] - [hist_{k0}(t-\Delta t)] \tag{3.18}$$

and analogous for $[hist_{m0}]$. Recursive updating is efficient here, in contrast to coupled inductances, because the branches consist only of capacitances here, unless currents are to be computed as well. In the latter case, $[i_{k0}(t)]$ is first found from Eq. (3.16), and then inserted into Eq. (3.17) to obtain the updated history term, with both formulas using the same matrix $1/\Delta t$ [C].

3.3.1 Error Analysis

The errors are the same as for the uncoupled capacitance, that is, the ratio $\tan(\omega \Delta t/2) / (\omega \Delta t/2)$ of Eq. (2.35) applies to every element in the matrix 1/2 [C]. The stub-line representation of Fig. 2.23 becomes an M-phase stub-line, with the second set of nodes being ground in this case. There is no need to use modal analysis, as explained in Section 3.2.1.

3.3.2 Damping of "Numerical Oscillations" with Series Resistances

Again, the explanations of Section 2.3.2 for the uncoupled capacitance are easily generalized to the matrix case if all elements of 1/2 [C] are to have the same time constant R_sC. Eq. (2.39) would then become

$$[R_s] = 0.15\ \Delta t[C]^{-1} \tag{3.19}$$

(factor 1/2 of Eq. (2.39) disappeared because the equations have been written for 1/2 [C] here). As mentioned in Section 2.3.2, numerical oscillations in capacitive currents have seldom been a problem.

3.3.3 Physical Reasons for Coupled Series Resistances

None are known to the writer at this time. The discussions of Section 2.3.3 do not apply to shunt capacitances of overhead lines, but they may be relevant to the capacitances of underground or submarine cables.

3.3.4 Example for Network with Coupled Capacitances

Assume that a power plant with a number of generator-transformer units in parallel is connected into the 230 kV switchyard through a number of parallel underground cables. The circuit breakers at the end of the cables are open, when a single-phase-to-ground fault occurs on the power plant side of the breakers (Fig. 3.11).

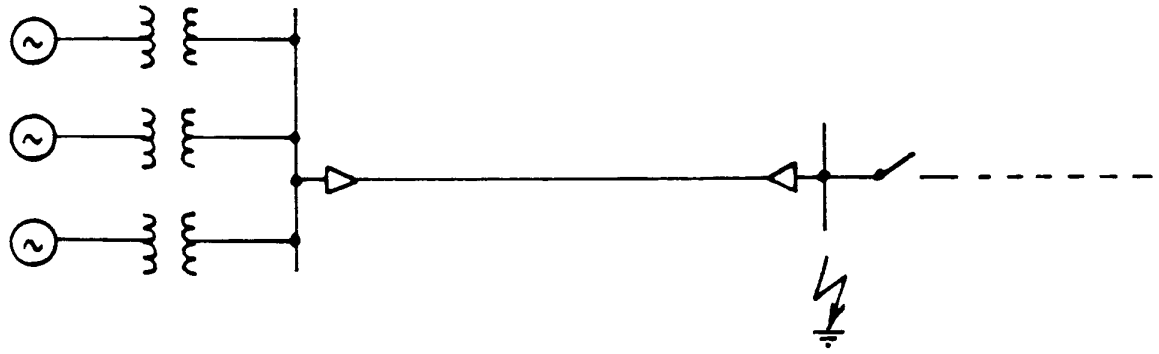

Fig. 3.11 - Cable circuit with single-phase-to-ground fault. Fault occurs in phase A when source voltage in A is at its peak. Generator-transformers represented as three-phase voltage sources of 230 kV (RMS, line-to-line) behind coupled reactances with $X_{pos} = 8\ \Omega$, $X_{zero} = 2.8\ \Omega$ (referred to 230 kV side). Cables represented as three-phase nominal π-circuit with $Z_{pos} = Z_{zero} = 0.015834\ \Omega$, $\omega C_{pos} = \omega C_{zero} = 897.6\ \mu S$, $R_{FAULT} = 1\ \Omega$

The data resembles the situation at Ground Coulee before the Third Powerhouse was built, except that $Z_{zero} = Z_{pos}$ for the cables is an unrealistic assumption. Also note that the shunt capacitances of the nominal π-circuit are actually uncoupled in this case because $C_m = 0$, which is always true in high voltage cables where each phase is electrostatically shielded. Nonetheless, this cable circuit was chosen because it illustrates the effects of shunt capacitances better than a case with overhead lines where $C_m \neq 0$.

Fig. 3.12(a) shows the voltages in the two unfaulted phases at the fault location, with oscillations superimposed on the 60 Hz so typical of cable circuits. Fig. 3.12(b) shows the fault current; the high-frequency oscillations at the beginning are caused by discharging the shunt capacitance through the fault resistance of 1 Ω. With zero fault resistance, this discharge would theoretically consist of an infinite current spike at $t = 0$, which leads to the undamped numerical oscillations across the correct 60 Hz - values discussed in Section 2.3.2 (Fig. 3.12(c)). These numerical oscillations would not appear if the cables were modelled as lines with distributed parameters; instead, physically based travelling wave oscillations would appear which would still look similar to those of Fig. 3.12(b).

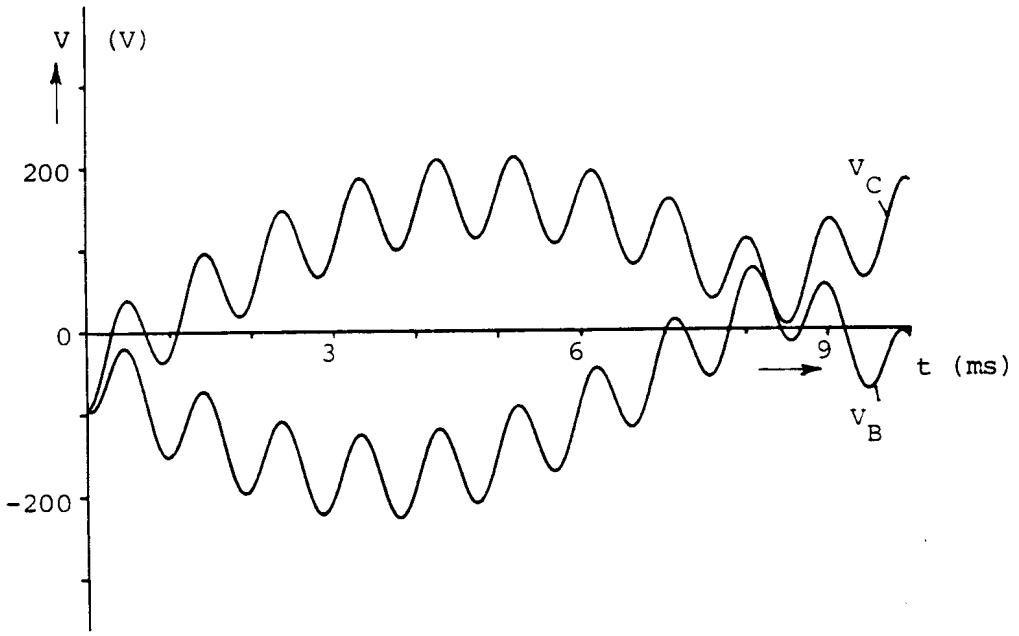

(a) Overvoltages

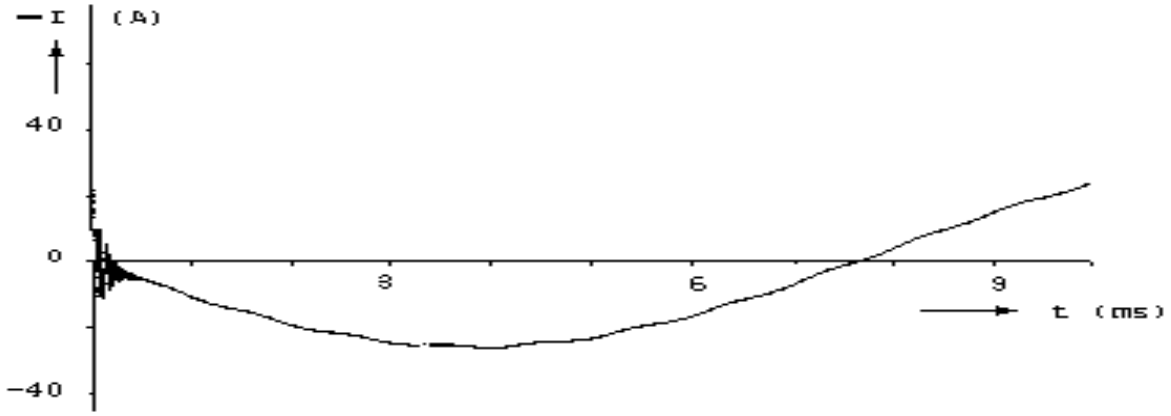

(b) Fault current for $R_{FAULT} = 1\ \Omega$ (negative value shown)

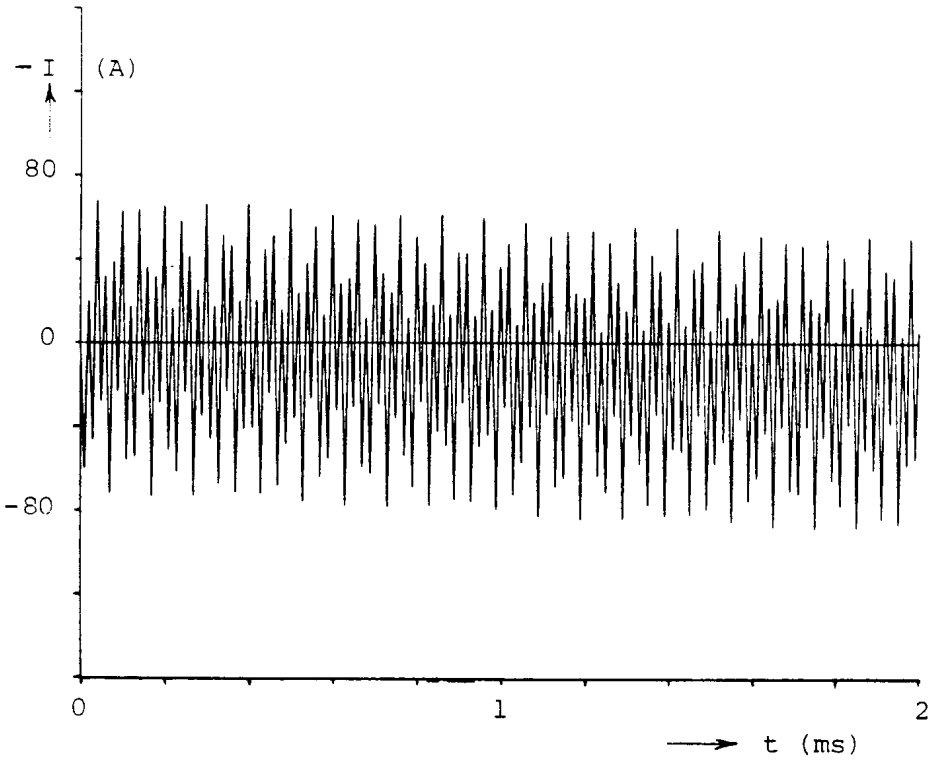

(c) Fault current for $R_{FAULT} = 0$ (different scale than in (b), but value again negative)

Fig. 3.12
- Overvoltages and fault current for a single-phase-to-ground fault in the cable circuit of Fig. 3.11 ($\Delta t = 10\mu s$; small step size chosen to allow comparisons with distributed parameter model of cable with $Z_{surge} = 4.2\Omega$, $\tau = 10\mu s$)

3.4 M-Phase Nominal π-Circuit

Series connections of coupled resistances and coupled inductances first appeared as part of M-phase nominal π-circuits (Fig. 3.10) when the EMTP was developed. It was therefore decided to handle such series connections as part of an M-phase nominal π-circuit input option. By allowing the shunt capacitance 1/2 [C] to be zero, this π-circuit input option can then be used for series connections of [R] and [L] as well.

The equations for the shunt capacitance matrices 1/2 [C] at both ends are solved as discussed in Section 3.3. [C] = 0 is not recognized by the EMTP as a special case; instead, the calculations are done as if [C[were nonzero.

What remains to be shown is the series connection of [R] and [L] as one single set of M coupled branches. The derivation of the coupled branch equations is similar to that of the scalar case discussed in Section 2.4, if scalar quantities are replaced by matrices. When the series [R] - [L] connection was first implemented in the EMTP, it was not recognized that [L] may not always exist. With the appearance of singular $[L]^{-1}$ matrices, e.g., in the transformer model of Eq. (3.3), an alternative formulation was developed. Both formulations have been implemented, as discussed in the next two sections.

3.4.1 Series Connection of [R] and [L]

For the steady-state solution, the branch equations are

$$I_{km} = \{[R] + j\omega[L]\}^{-1}\{[V_k] - [V_m]\} \tag{3.20}$$

They are solved accurately. For the transient simulation, the branch equations are derived by adding the voltage drops across [R] and [L]. From Eq. (3.2) and (3.8),

$$[i_{km}(t)] = [G_{series}]\{[v_k(t)] - [v_m(t)]\} + [hist_{series}(t-\Delta t)] \tag{3.21a}$$

with

$$[R_{series}] = [R] + \frac{2}{\Delta t}[L] \ , \quad and \quad [G_{series}] = [R_{series}]^{-1} \tag{3.21b}$$

and the history term

$$[hist_{series}(t-\Delta t)] = [G_{series}]\{[v_k(t-\Delta t)] - [v_m(t-\Delta t)] + \left(\frac{2}{\Delta t}[L] - [R]\right)[i_{km}(t-\Delta t)]\} \tag{3.22}$$

Direct updating of the history term with Eq. (3.22) involves three matrix multiplications because $[i_{km}]$ must first be found from Eq. (3.21a). Unless currents must be computed anyhow, as part of the output quantities, updating with the following recursive formula is more efficient,

$$[hist_{series}(t) = [H]\{[v_k(t)] - [v_m(t)] + [R_{series}][hist_{series}(t-\Delta t)]\} - [hist_{series}(t-\Delta t)] \tag{3.23a}$$

since it involves only two matrix multiplications. Matrix [H] is

$$[H] = 2\{[G_{series}] - [G_{series}][R][G_{series}]\} \tag{3.23b}$$

All matrices $[R_{series}]$, $[G_{series}]$ and [H] are still symmetric, which is exploited by the EMTP with the storage scheme discussed in the last paragraph before Section 3.1.1. Symmetry is not automatically assured. For instance, the alternative updating formula

$$[hist_{series}(t)] = [F][i_{km}(t)] - [hist_{series}(t-\Delta t)]$$

which, in combination with Eq. (3.21a), would be preferable in situations where current output is requested, has an unsymmetric matrix [F],

$$[F] = [H][R_{series}]$$

All equations in this section can handle the special case of either [R] = 0 or [L] = 0 as long as [R_{series}] of Eq. (3.21b) can be inverted.

3.4.2 Series Connections of [R] and $[L]^{-1}$

Singular matrices $[L]^{-1}$ appear in transformer representations if exciting currents are ignored. By itself, $[L]^{-1}$ is easily handled with Eq. (3.8) and (3.9). In series connections with [R], however, the equations of the preceding section cannot be used directly because [L] does not exist.

For the steady-state solution, the matrix [R] + jω [L] is rewritten as

$$[R] + j\omega[L] = [j\omega L]\{[j\omega L]^{-1}[R] + [U]\}$$

with [U] being the identity matrix, which upon inversion, produces the inverse required in Eq. (3.20),

$$\{[R] + j\omega[L]\}^{-1} = \{[U] + [j\omega L]^{-1}[R]\}^{-1}[j\omega L]^{-1} \tag{3.24}$$

Eq. (3.24) produces a symmetric matrix, even though the matrix [U] + $[j\omega L]^{-1}$[R] needed as an intermediate step is unsymmetric. The symmetry of the result from Eq. (3.24) can be shown by rewriting the matrix [R] + jω[L] as

$$[R] + j\omega[L] = [j\omega L]\{[j\omega L]^{-1}[R][j\omega L]^{-1} + [j\omega L]^{-1}\}[j\omega L]$$

from which the inverse is obtained as

$$\{[R]+j\omega[L]\}^{-1} = [j\omega L]^{-1}\{[j\omega L]^{-1}[R][j\omega L]^{-1} + [j\omega L]^{-1}\}^{-1}[j\omega L]^{-1} \tag{3.25}$$

Each of the three factors of the product is a symmetric matrix, which is obvious for the two outer factors and which can easily be proved for the inner factor by showing that its transpose is equal to the original. With all three factors being symmetric, the triple product [A][B][A] is symmetric, too. The EMTP uses Eq. (3.24) rather than (3.25), because the latter would fail if [R] = 0 and $[L]^{-1}$ singular. The EMTP does not use complex matrix inversion, followed by matrix multiplication with an imaginary matrix, however. Instead, Eq. (3.24) is reformulated as the solution of a system of N linear equations with N right-hand sides,

$$\{j[U] + [\omega L]^{-1}[R]\}[Y] = [\omega L]^{-1} \tag{3.26}$$

where the inverse [Y] is now directly obtained as the N solution vectors. To avoid complex matrix coefficients, Eq. (3.26) is further rewritten as 2N real equations,

$$[\omega L]^{-1}[R][Y_r] - [Y_i] = [\omega L]^{-1} \tag{3.27}$$

$$[Y_r] + [\omega L]^{-1}[R][Y_i] = 0 \tag{3.28}$$

By replacing $[Y_r]$ in Eq. (3.27) with the expression from Eq. (3.28), the imaginary part of [Y] is found by solving the N real equations

$$\left\{\left([\omega L]^{-1}[R]\right)^2 + [U]\right\}[Y_i] = -[\omega L]^{-1} \tag{3.29}$$

and the real part is then calculated from Eq. (3.28).

For the transient simulation, $[R_{series}]$ of Eq. (3.21b) is rewritten as

$$[R] + \frac{2}{\Delta t}[L] = \frac{2}{\Delta t}[L]\left\{\frac{\Delta t}{2}[L]^{-1}[R] + [U]\right\}$$

which, upon inversion, produces the matrix $[G_{series}]$ required in Eq. (3.21a),

$$[G_{series}] = \{[U] + \frac{\Delta t}{2}[L]^{-1}[R]\}^{-1}\frac{\Delta t}{2}[L]^{-1} \tag{3.30}$$

Again, the matrix $[U] + \Delta t/2\,[L]^{-1}[R]$ needed as an intermediate step is unsymmetric, while the final result $[G_{series}]$ becomes symmetric. Symmetry is proved with Eq. (3.25) by simply replacing $j\omega$ by $2/\Delta t$. As in the steady-state case, the inverse of Eq. (3.30) is found by solving N linear equations

$$\{[U] + \frac{\Delta t}{2}[L]^{-1}[R]\}[G_{series}] = \frac{\Delta t}{2}[L]^{-1} \tag{3.31}$$

To initialize the history term $[hist_{series}]$, Eq. (3.21a) can be used directly. To update it, neither Eq. (3.22) nor Eq. (3.23a) can be used because [L] and $[R_{series}]$ do not exist. Instead, Eq. (3.23a) is rewritten as

$$[hist_{series}(t)] = [H]\{[v_k(t)] - [v_m(t)]\} + [hist_{series}(t-\Delta t)] +$$

$$[G_{series}][-2R][hist_{series}(t-\Delta t)] \tag{3.32}$$

By storing the symmetric matrices [H], $[G_{series}]$ and -2[R], the updating with Eq. (3.32) can be done with three matrix multiplications, starting with the product $-2[R][hist_{series}(t - \Delta t)]$. An alternative updating formula, which requires the storage of only two symmetric matrices $[G_{series}]$ and -2[R], and produces the currents $[i_{km}]$ as a by-product, is

$$[hist_{series}(t)] = [G_{series}]\{[v_k(t)] - [v_m(t)] + [-2R][i_{km}(t)]\} + [i_{km}(t)] \tag{3.33}$$

if the current is first found from Eq. (3.21a), followed by the multiplication $-2[R][i_{km}(t)]$, etc. Eq. (3.33) is derived from Eq. (3.22) by rewriting $2/\Delta t$ [L] - [R] as $[R_{series}]$ -2[R].

All equations in this section have symmetric matrices, and can handle the special case of either [R] = 0 or $[L]^{-1} = 0$ as long as $[U] + \Delta t/2\,[L]^{-1}[R]$ in Eq. (3.30) can be inverted. Note, however, that $[L]^{-1} = 0$ implies infinite inductances, that is, the M coupled branches are really M open switches.